ARTICLE

OBC
www.rsc.org/obc

Reactivity of hydrazinophthalazine drugs with the lipid peroxidation products acrolein and crotonaldehyde

Lisa M. Kaminskas,[a,b] Simon M. Pyke[b] and Philip C. Burcham*[a]

[a] *Molecular Toxicology Research Group, Department of Clinical and Experimental Pharmacology, The University of Adelaide, Adelaide, SA 5005, Australia. E-mail: philip.burcham@adelaide.edu.au*

[b] *Department of Chemistry, The University of Adelaide, Adelaide, SA 5005, Australia*

Received 10th June 2004, Accepted 27th July 2004
First published as an Advance Article on the web 20th August 2004

The nucleophilic drug hydralazine strongly inhibits cell toxicity mediated by acrolein, a short chain 2-alkenal formed during lipid peroxidation. We here report the chemistry of acrolein-trapping by hydralazine, and show that together with its structural analogue dihydralazine, it also readily traps crotonaldehyde. Isolable reaction products included (1*E*)-acrylaldehyde phthalazin-1-ylhydrazone (*E*-APH), (1*Z*)-acrylaldehyde phthalazin-1-ylhydrazone (*Z*-APH), (1*E*,2*E*)-but-2-enal phthalazin-1-ylhydrazone (*E*-BPH) and (1*Z*,2*E*)-but-2-enal phthalazin-1-ylhydrazone (*Z*-BPH). Concentration-dependent formation of (1*E*)-acrylaldehyde phthalazin-1-ylhydrazone was observed in the culture media of cells co-exposed to hydralazine and the acrolein precursor allyl alcohol. These aldehyde-sequestering properties of hydrazinophthalazine drugs may contribute to the protection they provide against 2-alkenal-mediated toxicity.

Introduction

Lipid peroxidation accompanies many debilitating health conditions including inflammatory disorders,[1] cardiovascular disease,[2,3] neurodegenerative conditions[4–6] and diabetes.[7] Such oxidative fragmentation of unsaturated lipids generates multiple reactive carbonyls including malondialdehyde, various 4-hydroxy-2-alkenals, and a range of 2-alkenals such as acrolein **1** and crotonaldehyde **2**.[3,8–9] Acrolein **1** is also a ubiquitous environmental pollutant due to its formation during the combustion of organic matter.[10–11] A potent electrophile, acrolein **1** readily forms adducts in biological macromolecules such as DNA and protein, thereby disrupting a wide range of cellular processes. Acrolein-adducted proteins have been detected in the affected tissues of several chronic degenerative diseases known to involve oxidative stress, including Alzheimer's disease[12] and diabetic kidney disease.[13]

Given this contribution of short-chain 2-alkenals to oxidative cell injury, our laboratory began a search for nucleophilic drugs that attenuate the toxicity of these substances.[14,15] The goal is to identify nucleophilic compounds that react with toxic carbonyls at a faster rate than do cell macromolecules, sparing the latter and ensuring carbonyls are excreted as drug-carbonyl derivatives.[15,16] Other laboratories have identified various compounds that scavenge sugar-derived carbonyls, and several of these have also been shown to trap lipid-derived substances.[15,17–23] To date, however, few non-thiol compounds with efficient trapping-activity towards short-chain 2-alkenals such as acrolein **1** and crotonaldehyde **2** have been described.

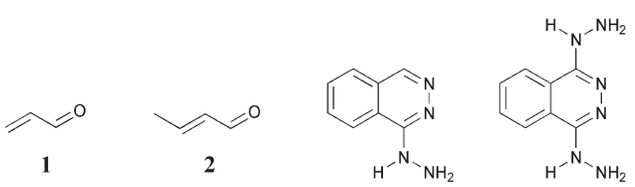

1 **2** **3** **4**

In the present work, we compared the 2-alkenal-trapping potencies of various carbonyl-sequestering compounds to those of hydralazine **3**, a vasodilatory antihypertensive that is one of the strongest nucleophiles in clinical use.[24] Possessing a reactive hydrazine group, hydralazine **3** traps a wide range of biogenic keto compounds, including pyruvate, acetate and 2-ketoglutarate.[25] Formation of a hydrazone with pyruvate is a major metabolic fate of hydralazine in human subjects.[25] In the present work, we provide evidence that hydralazine **3** and its structural analogue dihydralazine **4** display much stronger 2-alkenal-trapping potency than several other nucleophilic amines previously identified as scavengers of lipid-derived aldehydes. The protection these drugs afford against the toxicity of 2-alkenals may involve an ability to minimise adduction of cell constituents *via* this mechanism.

Results and discussion

2-Alkenal-trapping potencies of various nucleophiles in solution

The acrolein-sequestering efficacy of the various nucleophilic compounds varied significantly over the course of 30 min reactions at 37 °C and neutral pH (Fig. 1A). Somewhat surprisingly, the advanced glycation end product (AGE) inhibitor aminoguanidine **5** displayed little or no acrolein-trapping potency (Fig. 1A). Aminoguanidine has been investigated in clinical trials with diabetic subjects due to its potency as an inhibitor of AGE formation.[17,18,26] While aminoguanidine readily scavenges Amadori fragmentation products and blocks protein modification by the open-chain form of sugars, it also readily traps two important lipid-derived α,β-unsaturated aldehydes, malondialdehyde and 4-hydroxy-2-nonenal.[18] Given that both malondialdehyde and 4-hydroxy-2-nonenal contain a β-hydroxy group, the minimal reactivity of aminoguanidine with acrolein we observed may suggest unsaturated aldehydes possessing a β-hydroxy group are most reactive with this drug.

The endogenous AGE inhibitor carnosine **6** traps 2-*trans*-hexenal and 4-hydroxy-2-nonenal and also blocks protein adduction by malondialdehyde;[19–22] while pyridoxamine **7** traps 9- and 13-keto-octadecadienoic acids.[23] Both pyridoxamine and carnosine reacted only slowly with acrolein, removing 28 and 29% respectively of the aldehyde from solution over a 30 min period (Fig. 1A). Methoxyamine **8**, a versatile carbonyl-trapping reagent, also displayed only modest reactivity with acrolein (Fig. 1A). The clinically used acrolein-trapping thiol MESNA (sodium 2-mercaptoethanesulfonate) **9** sequestered almost all the free acrolein within 10 min (Fig. 1A). This is consistent with the observation that thiol-containing nucleophiles add rapidly to the β-carbon of acrolein, forming stable thioether conjugates.[8] Hydralazine **3** and dihydralazine **4** also displayed very strong acrolein-trapping reactivity, respectively diminishing free acrolein concentrations to 8 and 1% of initial acrolein concentrations after

DOI: 10.1039/b408796h

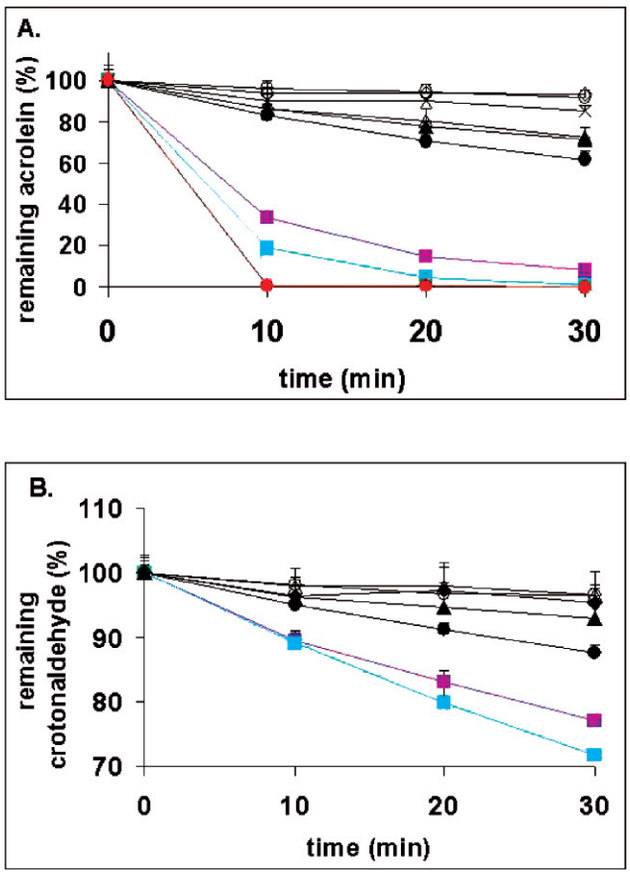

Fig. 1 Disappearance of free acrolein **1** (Panel A) or crotonaldehyde **2** (Panel B) from buffered solutions at neutral pH and 37 °C in the presence of equimolar concentrations of various nitrogen-containing nucleophiles (Panels A and B) and the sulfur nucleophile MESNA (Panel A only). At each time point, free **1** or **2** concentrations were measured in reaction mixture aliquots using UV-HPLC. The starting concentration of aldehydes and nucleophilic compounds was 0.5 mM. Aldehyde concentrations remaining at each time point are expressed as a percentage of starting concentrations. The various treatments shown are: control (buffer + 2-alkenal only, ◇); hydralazine **3** (magenta ■), dihydralazine **4** (blue ■), aminoguanidine **5** (○), carnosine **6** (▲), pyridoxamine **7** (△), methoxyamine **8** (●), and MESNA **9** (red ●). Each data point represents the mean of 3 independent observations (±S.E.).

30 min (Fig. 1A). Nevertheless, although the rate of acrolein consumption by the hydrazino drugs clearly exceeded that of the other nitrogen-containing nucleophiles, it was less than that exhibited by MESNA **9**.

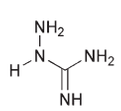

5

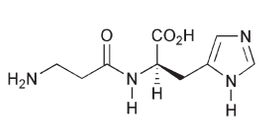

6

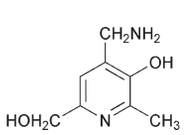

7

8

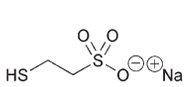

9

In terms of ranking, the reactivity of the various nitrogen-containing nucleophilic scavengers towards **2** resembled that seen with **1** (Fig. 1B), although the rate of the reaction with **2** was typically slower than that with **1** (note the altered *Y*-axis in Fig. 1B). Hydralazine **3** and dihydralazine **4** again displayed greater reactivity with crotonaldehyde than any of the other amine compounds studied (Fig. 1B).

Characterisation of reaction products

We then sought to characterize products formed during reactions between hydralazine and acrolein or crotonaldehyde. ^{1}H NMR analysis of products isolated from reactions between **1** and **3** identified a yellow crystalline hydrazone product eluting at a high R_f as (1*E*)-acrylaldehyde phthalazin-1-ylhydrazone, *E*-APH, **10** (35% yield). An additional low R_f reaction product was determined by ^{1}H NMR to be (1*Z*)-acrylaldehyde phthalazin-1-ylhydrazone, *Z*-APH, **11** (4% yield). The stereochemistry of the hydrazones was determined by the downfield shift of the C1 proton; *c.f.* δ 8.10 for **10** *vs.* δ 7.36 for product **11** (the downfield shift identifies the *E*-isomer).[27] Product **11** showed poor stability and we were unable to purify this product completely. Another problem encountered during the study of reactions between **1** and **3** was the formation of a precipitate in some vials. During ^{1}H NMR analysis of this material, spectra with similar features to those seen with APH were observed, including signals in the vinylic and aryl regions (spectra not shown). ESI-MS analysis suggested the presence of oligomeric forms of APH, with ions detected at *m*/*z* 199, 397 and 595 (spectra not shown).

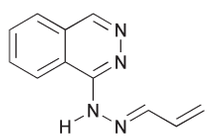

10 *E*-APH

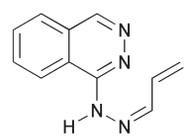

11 *Z*-APH

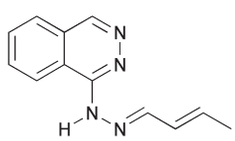

12 *E*-BPH

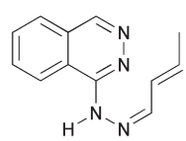

13 *Z*-BPH

Two products were also formed during reactions between **2** and **3**, namely (1*E*,2*E*)-but-2-enal phthalazin-1-ylhydrazone, *E*-BPH (34% yield) **12**, and its isomer (1*Z*,2*E*)-but-2-enal phthalazin-1-ylhydrazone, *Z*-BPH (6% yield) **13**. Again, determination of hydrazone stereochemistry was achieved by comparison of the chemical shifts of the C1 proton; δ 8.05 for **12** *vs.* δ 7.32 for **13** (again the downfield shift identifies the *E*-isomer). Upon prolonged standing of the individual isomers in deuterated chloroform for several weeks at 4 °C, **13** equilibrated to **12**, whereas **12** did not equilibrate appreciably to **13**. This suggests that **13** is the kinetic product of reactions between crotonaldehyde and hydralazine whereas **12** is the thermodynamic product.

Kinetics of reactions between 2-alkenals and hydralazine

Since efforts to synthesise *E*-APH **10** resulted in quite low yields, the kinetics and stability of this material was explored. HPLC was used to monitor the kinetics of **10** formation in a 1 : 1 ratio of **3** and **1** in buffered solution at 37 °C (Fig. 2A) and 4 °C (Fig. 2B). The reactions were studied at both temperatures to address the possibility that side-reactions (*e.g.* formation of polymeric species) could be minimized at low temperatures. The low R_f product formed during reactions between **1** and **3** was not monitored as it formed a broad asymmetric peak during HPLC analysis. Also, this material could not be purified in sufficient quantities to obtain the molar absorptivity for use in construction of standard curves. In contrast to the 35% yield obtained during the synthesis of **10** described under the "Characterisation of reaction products" section above, the lower concentration of reagents used in the kinetic study (500 μM for both acrolein and hydralazine) gave **10** in approx. 10% yield after 24 h at either 37 °C or 4 °C (Figs. 2A and B, respectively). The low yield was not due to product instability, since **10** alone was stable in solution over a 24 h period at 4 °C, although some loss of **10** was evident with prolonged incubation at 37 °C. The kinetics of **1**

consumption during the reaction revealed greater loss of aldehyde than was expected on the basis of the 1 : 1 stoichiometry predicted during reactions between **1** and **3** (Figs. 2A and B). Acrolein loss due to self-condensation or evaporation did not cause this discrepancy, since solutions of **1** alone were very stable under the same conditions in the absence of drug (Figs. 2A and B). Thus **3** appeared to facilitate acrolein consumption *via* pathways in addition to direct 1 : 1 trapping, a conclusion consistent with the ESI-MS data mentioned above which suggested the formation of oligomeric products. Thus **10** may be a precursor for the oligomeric products that eluted poorly from silica columns. Due to the difficulties involved in extracting these products, we were unable to determine their yield during the kinetic experiments.

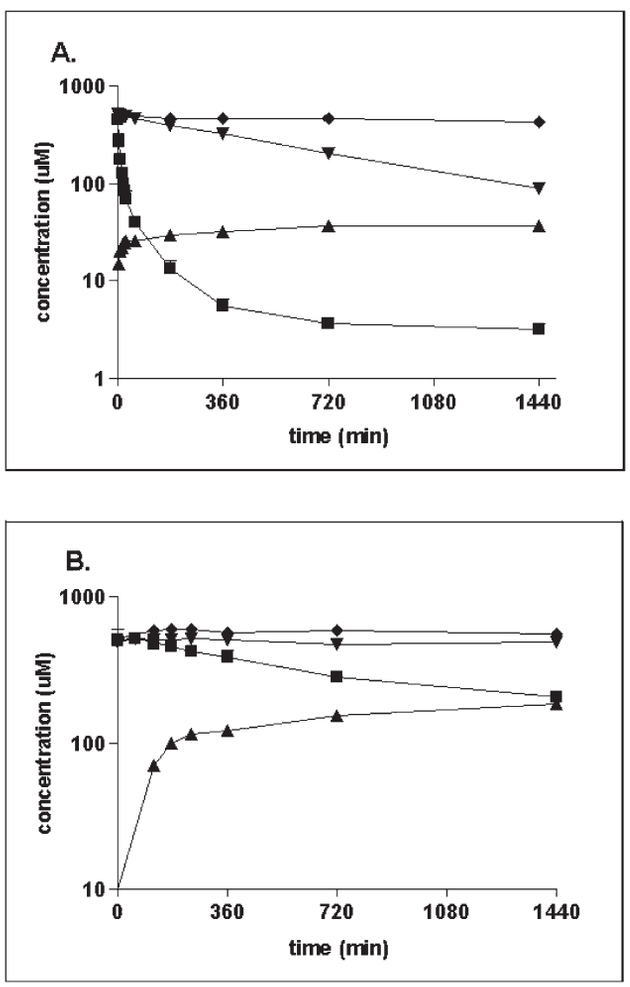

Fig. 2 The kinetics of *E*-APH **10** formation (▲) and acrolein **1** disappearance (■) in equimolar mixtures of **1** and hydralazine **3** (500 μM) in buffered solution at neutral pH and 37 °C (Panel A) or 4 °C (Panel B). Panels A and B also depict the stability of solutions of **1** only (▼) or **10** only (◆) in buffer during extended incubation at the respective temperatures. Levels of **10** and **1** were measured *via* UV-HPLC as described in the experimental section. Each point represents the mean ± S.E. of 3 independent observations.

We also monitored the kinetics of *E*-BPH **12** formation from **2** and **3**. As with the low R_f product formed during reactions between acrolein and hydralazine, *Z*-BPH **13** could not accurately be measured by HPLC as it eluted as a very broad peak that could not be reproducibly quantified. As predicted on the grounds of the earlier experiments (Fig. 1), *E*-BPH **12** formed more slowly than *E*-APH **10**, although the yield after 24 h was considerably higher: 47% at 37 °C (Fig. 3A) and 63% at 4 °C (Fig. 3B) respectively. The higher yields may indicate a lesser tendency towards the formation of oligomers from **3** compared to **1**. Reactions were complete after 6 h at 37 °C, after which **12** concentrations began to decline, although when performed at 4 °C, the trapping reaction between **3** and **2** had not reached equilibrium even after 24 h (Fig. 3B).

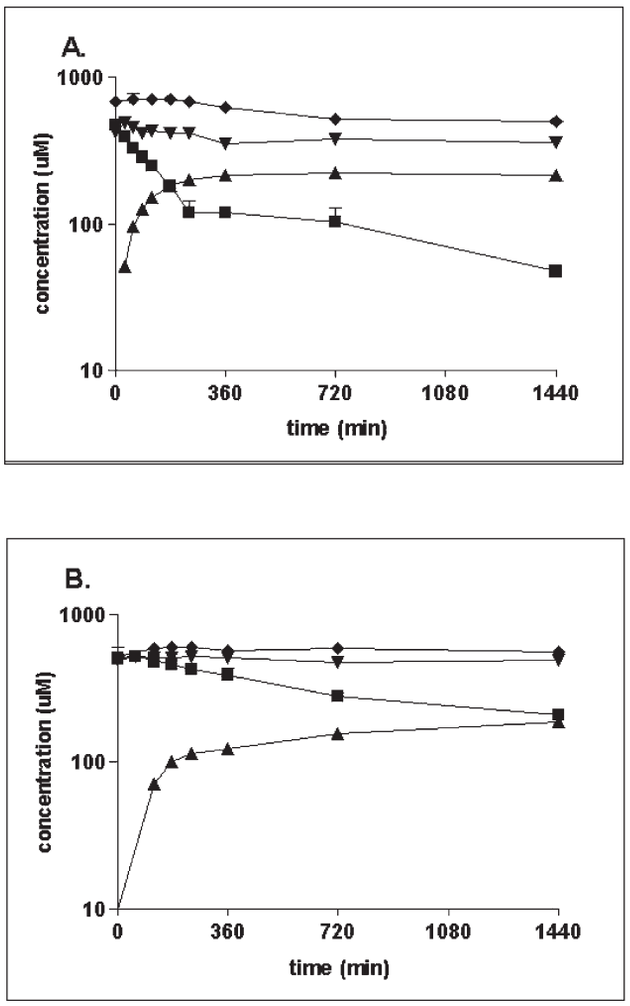

Fig. 3 The kinetics of *E*-BPH **12** formation (▲) and crotonaldehyde **2** disappearance (■) in equimolar mixtures of **2** and hydralazine **1** (500 μM) in buffered solution at neutral pH and 37 °C (Panel A) or 4 °C (Panel B). Panels A and B also depict the stability of solutions of **2** only (▼) or **12** only (◆) in buffer during extended incubation at each temperature. Levels of **12** and **2** were measured *via* UV-HPLC as described in the experimental section. Each data point represents the mean ± S.E. of 3 independent observations.

Cytoprotection against 2-alkenal-mediated toxicity in isolated hepatocytes

To assess whether the hydrazone-forming properties of hydrazino drugs are relevant in a cellular model, we compared the ability of **3** and **4** to attenuate the toxicity of unsaturated alcohol precursors to 2-alkenals in isolated mouse hepatocytes. Alcohol dehydrogenase-rich hepatocytes readily convert allyl and crotyl alcohols to their respective oxidation products, **1** and **2**.[27,28] Both alcohols produce time- and concentration-dependent cell killing in mouse hepatocytes, preceded by extensive GSH depletion and protein carbonylation, effects that are abolished by alcohol dehydrogenase inhibitors.[27,29] For the present experiments, mouse hepatocytes were exposed to either 100 μM allyl alcohol (Fig. 4) or 500 μM crotyl alcohol (Fig. 5) in the presence of 0 to 100 μM concentrations of either hydralazine **3** ("A" panels in Figs. 4 and 5) or dihydralazine **4** ("B" panels in Figs. 4 and 5). Exposure to the unsaturated alcohols alone was very toxic to the cells, inducing almost maximal cell death within 2 h ("A" panels in Figs. 4 and 5). Micromolar concentrations of hydralazine **3** and dihydralazine **4** afforded clear, concentration-dependent protection against the toxicity of both allyl and crotyl alcohols. To enable comparison between the various sets of data, the LDH leakage curves obtained in the presence of the respective alcohol and 10 (pink ▲) and 30 (blue ●) μM concentrations of each hydrazine drug are labeled with the same colour in each panel of Figs. 4 and 5. In keeping with its possession of two nucleophilic hydrazine substituents and greater

reactivity with aldehydes, **4** was approximately twice as cytoprotective as **3** against the toxicity of both alcohols. Both arylhydrazine drugs afforded stronger cytoprotection against allyl alcohol toxicity than MESNA **9**, which provided only minimal protection at 100 μM (data not shown). Since MESNA **9** was a highly efficient acrolein-trapping reagent (Fig. 1), its lesser cytoprotective potency in hepatocytes presumably reflects poor cellular access due to low lipophilicity. This concurs with clinical observations during the use of **9** to control acrolein-mediated bladder injury in chemotherapy patients, since following administration by the intravenous route, **9** is predominantly retained within the intravascular space and only protects against hemorrhagic cystitis.[30]

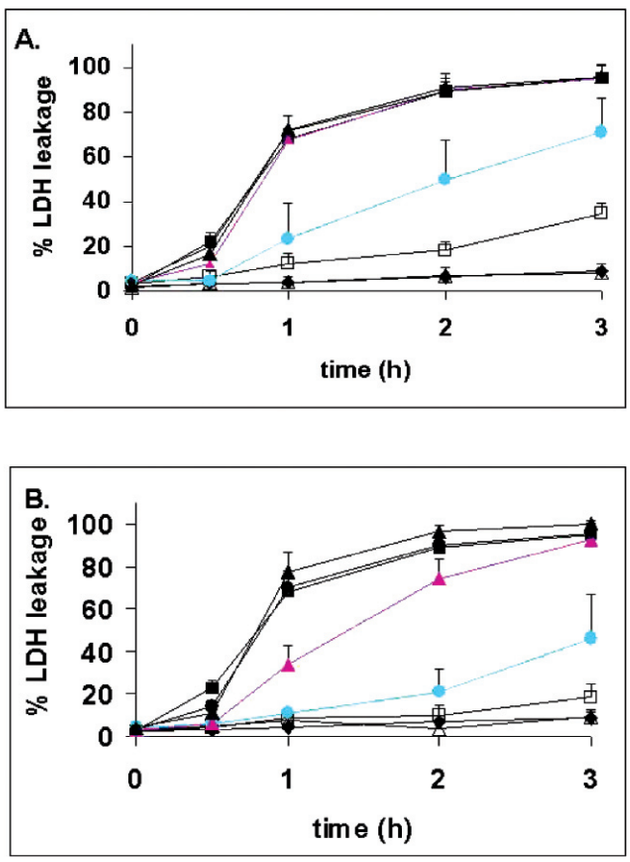

Fig. 4 Concentration-dependent protection against the toxicity of allyl alcohol in primary cultured mouse hepatocytes by 1 to 100 μM concentrations of hydralazine **3** (Panel A) or dihydralazine **4** (Panel B). The various treatments shown are: controls (media alone, ◆); 100 μM respective drug **3** or **4** only (△); 100 μM allyl alcohol (AA) only (■); AA + 1 μM drug (●); AA + 3 μM drug (▲); AA + 10 μM drug (pink ▲); AA + 30 μM drug (blue ●); AA + 100 μM drug (□). LDH leakage into the culture medium was used as an indicator of cell death over a 3 h period. Each data point represents the mean ± S.E. of 3 independent observations.

Hydrazone formation in mouse hepatocytes

To confirm that acrolein **1** scavenging accompanied hydralazine and dihydralazine-induced cytoprotection, we measured total cellular *E*-APH **10** levels *via* UV-HPLC after 30 min exposure of hepatocytes to allyl alcohol (100 μM) and hydralazine **3** (0–100 μM). The 30 min time point was used since in mouse hepatocytes exposed to 100 μM allyl alcohol, **1** concentrations in extracellular media peak at approximately 4 μM at this time (P. C. Burcham, unpublished observation). This extent of **1** formation from allyl alcohol concurs with a reported 5% yield of free **1** in rat liver homogenates.[31] In the presence of hydralazine **3** and allyl alcohol, cellular *E*-APH **10** levels were below quantifiable levels at drug concentrations of 10 μM and below, although concentration-dependent acrolein-trapping was evident at 25, 50 and 100 μM drug concentrations, yielding respective cellular **10** levels of 39 ± 37, 121 ± 55 and 381 ± 97 pmol mL^{-1} (mean ± S.E., $N = 3$). These yields of **10** are consistent with the likelihood that "free" **1** concentrations in these cells may not exceed 4%

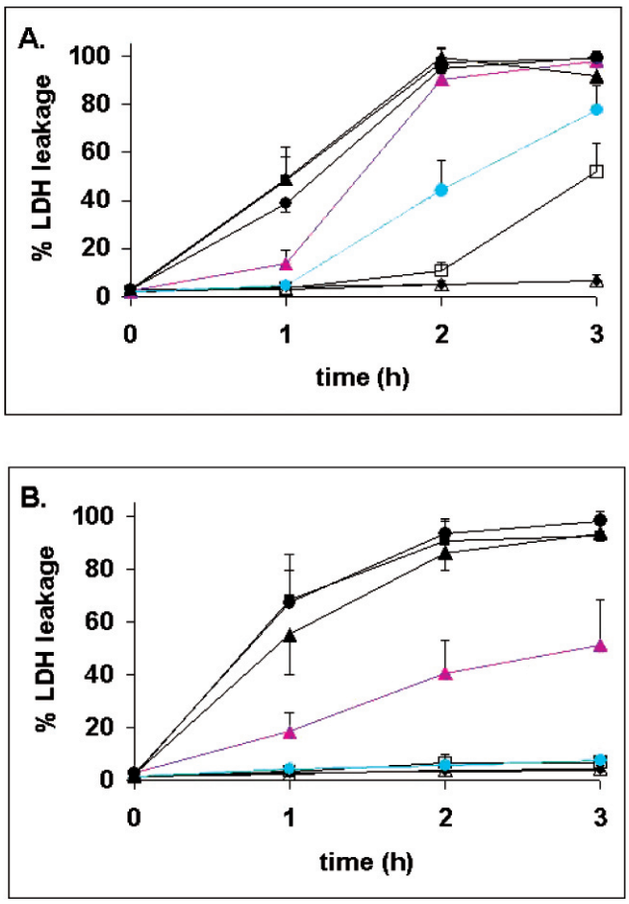

Fig. 5 Concentration-dependent protection against the toxicity of crotyl alcohol in primary cultured mouse hepatocytes by 1 to 100 μM concentrations of hydralazine **3** (Panel A) or dihydralazine **4** (Panel B). The various treatments shown are: controls (media alone, ◆); 100 μM respective drug **3** or **4** only (△); 500 μM crotyl alcohol (CA) only (■); CA + 1 μM drug (●); CA + 3 μM drug (▲); CA + 10 μM drug (pink ▲); CA + 30 μM drug (blue ●); CrOH + 100 μM drug (□). LDH leakage into the culture medium was used as an indicator of cell death over a 3 h period. Each data point represents the mean ± S.E. of 3 independent observations.

of the starting allyl alcohol concentration, and that the efficiency of 1 : 1 stoichiometry during acrolein-trapping by **3** may not exceed 10%. Another possible contributor to the low yield of **10** could be that cells rapidly metabolize this species. To address this possibility, we examined the levels of total **10** (*i.e.* levels in culture media plus cell lysates) over a 3 h period following its addition to the culture media of mouse hepatocytes to give a starting concentration of 1000 pmol mL^{-1}. After 30 min, total *E*-APH **10** levels had declined by over 90% to just 84 ± 40 pmol mL^{-1}, while by 60 min they were below detectable limits (mean ± S.E., $N = 3$). This suggests that at low **10** concentrations relevant to those likely to form in cells, **10** is rapidly removed, presumably *via* metabolic clearance.

Toxic potential of *E*-APH in isolated hepatocytes

Since it possesses an unsaturated center, the product of 1 : 1 acrolein-trapping by hydralazine, *E*-APH **10**, is potentially a reactive entity that may be targeted by nucleophiles in cellular macromolecules. We therefore addressed the issue of whether **10** represents a true detoxication product by examining its ability to induce toxicity in mouse hepatocyte monolayers. Toxicity was assessed by following cellular lactate dehydrogenase (LDH) leakage over 3 h in the presence of 0, 1 or 10 μM **10**. While the lowest concentration of **10** (1 μM) produced no change over control values by 3 h, 10 μM **10** modestly increased LDH leakage at this time (23 ± 6% compared to 10 ± 2% in controls). These findings suggest that at the submicromolar concentrations formed during intracellular trapping reactions, **10** is unlikely to induce cellular damage, suggesting this species constitutes a genuine detoxication product. Further studies are planned to characterize the metabolic and biological fate of **10**.

Conclusion

The current study provides confirmation that hydralazine **3** and its analogue dihydralazine **4** are efficient scavengers of toxic short-chain 2-alkenals, forming hydrazone derivatives in a rapid reaction at neutral pH. Consistent with these properties, **3** and **4** also provided strong protection against the cellular toxicity of unsaturated alcohol precursors to **1** and **2**. The findings suggest arylhydrazino drugs may be useful research tools for exploring the contribution of short-chain 2-alkenals to oxidative cell injury.

Experimental section

General

Melting points were recorded on a Reichert hot stage apparatus. ^{1}H and ^{13}C spectra were measured using either a Varian Gemini-2000 spectrometer (^{1}H 300 MHz, ^{13}C 75 MHz) or a Varian INOVA spectrometer (^{1}H 600 MHz, ^{13}C 150 MHz). The multiplicities of signals are reported as being: s, singlet; d, doublet; t, triplet; q, quartet; multiplet, an unassignable multiplicity or overlapping signals; br, broadened signal. Infra-red spectra were recorded on an ATI Mattson Genesis series FTIR™ as nujol mulls on sodium chloride plates. Ultraviolet spectra were recorded on a PYE Unicam SP8-100 ultraviolet spectrophotometer. ESI mass spectra were measured on a Finnigan LCQ spectrometer with the spray voltage set at 4.8 kV and a capillary temperature of 200 °C. EI mass spectra were performed by the Central Science Laboratory, University of Tasmania.

Thin layer chromatography (t.l.c.) was performed using Merck aluminium backed silica gel 60 F_{254} sheets. Flash column chromatography was performed using Merck silica gel 60 (particle size: 0.04–0.063 mm (230–400 mesh ASTM)). All solvents used for chromatography were distilled before use.

Male Swiss mice, aged 4–8 weeks, were obtained from Laboratory Animal Services at the University of Adelaide (Waite campus) and housed in a temperature-controlled room (21 °C) on a 12 h light/dark cycle. The Animal Ethics Committee at the University of Adelaide approved all animal experimentation reported in this manuscript.

To assess aldehyde sequestering by nucleophilic drugs, amine nucleophiles were dissolved in prewarmed sodium phosphate buffer (pH 7.0) to give a final concentration of 1 M before 0.5 mL volumes of these solutions were added to triplicate 1 mL gas chromatography vials. Reactions were started by the addition of prewarmed 0.5 mL volumes of equimolar concentrations of either **1** or **2** (1 M). Vessels were filled to capacity to minimize headspace loss of aldehydes (see below). The vials were then placed in a 37 °C mixing incubator for 10, 20 or 30 min. At each time point, an aliquot was taken from one of the triplicate vials, diluted 1 : 10 to 1 : 50 in mobile phase before a 100 μL sample was used for the determination of aldehyde concentrations *via* HPLC.

The HPLC system comprised an ODS Hypersil column (150 × 4.6 mm, 5 μm, Keystone Scientific Inc, PA, USA) connected to a GBC LC1150 pump (Dandenong, Australia), fitted with an online ERC 3415 degasser and a Hewlett Packard series 1100 UV detector that monitored the absorbance of column eluate at 210 nm. The mobile phase used to analyse free acrolein comprised 20% methanol/water (v/v) while in the case of crotonaldehyde, 30% methanol/water (v/v) was used. The flow rate was maintained at 1 mL min^{-1}. Under these conditions, the retention times for **1** and **2** were 2.7 and 3.1 min, respectively. Aldehyde concentrations were determined by comparing sample peak areas to those obtained by analysing standard solutions of **1** and **2** (prepared in mobile phase to give final aldehyde concentrations ranging from 0.1 to 12 μM.

(1*E*)-Acrylaldehyde phthalazin-1-ylhydrazone 10 and (1*Z*)-acrylaldehyde phthalazin-1-ylhydrazone 11

To prepare the main isolable product formed during trapping reactions, a 1 : 1 mixture of **3** and **1** (135 mM, 20 mL) in 50 mM sodium phosphate buffer (pH 7.0) was stirred for 1 h at 4 °C. The mixture was then extracted with chloroform (3 × 15 mL). The combined organic extracts were washed with brine (1 × 20 mL) and the organic layer dried over $MgSO_4$. This was then filtered and evaporated to dryness. The resulting oil was chromatographed on silica (20 × 3 cm flash column) using 1 : 20 ethyl acetate : dichloromethane as eluant. Thin layer chromatography (1 : 20 ethyl acetate : dichloromethane) revealed that the yellow crystalline substance recovered from acrolein–hydralazine reaction mixtures comprised two compounds, a low R_f component (approx. 10%) and a high R_f component (approx. 90%). The high R_f component could be isolated by preparative TLC (20 × 20 cm plate, 3 elutions with dichloromethane) and was found to be (1*E*)-acrylaldehyde phthalazin-1-ylhydrazone **10**, (32%, mp 61–63 °C). λ_{max}(CH_3CN)/nm 202 (log ε 5.0), 287 (4.3), 356 (4.2); ν_{max}(nujol)/cm^{-1} 3390 (NH), 3257 (ArH), 1624 (C=N), 1589 (C=C); δ_H (600 MHz; $CDCl_3$; Me_4Si) 5.58 [1 H, dt, $J_{2,3b}$ 10.3 $J_{1,3b}$ 1.1 $J_{3a,3b}$ 1.1, C(3)H_b], 5.61 [1 H, ddd, $J_{2,3a}$ 17.4 $J_{1,3a}$ 1.1 $J_{3a,3b}$ 1.1, C(3)H_a], 6.59 [1 H, ddd, $J_{1,2}$ 9.7 $J_{2,3a}$ 17.4 $J_{2,3b}$ 10.3, C(2)H], 7.41–7.43 [1 H, m, C(5′)H], 7.54–7.59 [2 H, m, C(6′,7′)H], 7.76 [1 H, s, C(4′)H], 8.10 [1 H, dt, $J_{1,2}$ 9.7 $J_{1,3a}$ 1.1 $J_{1,3b}$ 1.1, C(1)H], 8.27–8.29 [1 H, m, C(8′)H], 10.50 [1 H, br s, NH]; δ_C (150 MHz; $CDCl_3$; Me_4Si) 124.21 [C(8′)], 124.75 [C(3)], 126.04 [C(5′)], 126.53 [C(8a′)], 127.31 [C(4a′)], 131.61 [C(7′)], 132.12 [C(6′)], 135.07 [C(2)], 138.17 [C(4′)], 149.15 [C(1′)], 156.62 [C(1)]. *m*/*z* (EI): 199.0908 ($M^{+\bullet}$, $C_{11}H_{10}N_4$ requires 198.0905), 182 (22%), 171 (100).

The low R_f component was found to be (1*Z*)-acrylaldehyde phthalazin-1-ylhydrazone **11**. δ_H (600 MHz; $CDCl_3$; Me_4Si) 5.56 [1 H, dt, $J_{2,3b}$ 10.3 $J_{1,3b}$ 1.1 $J_{3a,3b}$ 1.1, C(3)H_b], 5.60 [1 H, ddd, $J_{2,3a}$ 17.4 $J_{1,3a}$ 1.1 $J_{3a,3b}$ 1.1, C(3)H_a], 7.36 [1 H, dt, $J_{1,2}$ 9.4 $J_{1,3a}$ 1.1 $J_{1,3b}$ 1.1, C(1)H], 7.40–7.42 [1 H, m, C(5′)H], 7.50 [1 H, ddd, $J_{1,2}$ 9.4 $J_{2,3a}$ 17.4 $J_{2,3b}$ 10.3, C(2)H], 7.54–7.59 [2 H, m, C(6′,7′)H], 7.75 [1 H, s, C(4′)H], 8.31–8.33 [1 H, m, C(8′)H], 10.44 [1 H, br s, NH]; δ_C (150 MHz; $CDCl_3$; Me_4Si) 124.34 [C(8′)], 124.97 [C(3)], 125.97 [C(5′)], 126.93 [C(8a′)], 127.51 [C(4a′)], 128.52 [C(2)], 131.48 [C(7′)], 131.99 [C(6′)], 138.07 [C(4′)], 148.35 [C(1′)], 153.87 [C(1)]. This component could not be isolated in a pure form and showed poor stability.

(1*E*,2*E*)-But-2-enal phthalazin-1-ylhydrazone 12 and (1*Z*,2*E*)-but-2-enal phthalazin-1-ylhydrazone 13

To characterize products formed during reactions between **3** and **2**, a 1 : 1 mixture of **3** and **2** (135 mM, 20 mL) in 50 mM sodium phosphate buffer (pH 7.0) buffer was stirred for 1 h at 4 °C. The mixture was then extracted with chloroform (3 × 15 mL) and the combined organic extracts were then washed with brine (20 mL) before they were dried over $MgSO_4$. Following filtration and evaporation to dryness, the reaction product was chromatographed on silica using 1 : 30 ethyl acetate : dichloromethane as eluant. Once again, two products were isolated; a yellow crystalline high R_f product and a yellow-brown solid low R_f product. The structure of the high R_f product was found to be (1*E*,2*E*)-but-2-enal phthalazin-1-ylhydrazone **12**, (34%, mp 111–114 °C). λ_{max}(CH_3CN)/nm 206 (log ε 4.6), 288 (4.4), 360 (4.3); ν_{max}(nujol)/cm^{-1} 3263 (NH), 1641 (C=N), 1607 and 1590 (C=C); δ_H (600 MHz; $CDCl_3$; Me_4Si) 1.81 [3 H, dd, $J_{2,4}$ 1.5 $J_{3,4}$ 6.9, C(4)H], 6.11 [1 H, dq, $J_{2,3}$ 15.3 $J_{3,4}$ 6.9, C(3)H], 6.31 [1 H, ddq, $J_{1,2}$ 9.6 $J_{2,3}$ 15.3 $J_{2,4}$ 1.5, C(2)H], 7.49–7.51 [1 H, m, C(5′)H], 7.62–7.67 [2 H, m, C(6′,7′)H], 7.83 [1 H, s, C(4′)H], 8.05 [1 H, d, $J_{1,2}$ 9.6, C(1)H], 8.35–8.36 [1 H, m, C(8′)H], 10.48 [1 H, br s, NH]; δ_C (150 MHz; $CDCl_3$; Me_4Si) 18.54 [C(4)], 123.95 [C(8′)], 125.83 [C(5′)], 126.65 [C(8a′)], 127.13 [C(4a′)], 129.90 [C(2)], 131.31 [C(7′)], 131.72 [C(6′)], 137.69 [C(4′)], 138.42 [C(3)], 148.36 [C(1′)], 156.60 [C(1)]; *m*/*z* (EI): 212.1063 ($M^{+\bullet}$, $C_{12}H_{12}N_4$ requires 212.1062), 197 (100%), 171 (29).

The low R_f component was found to be (1*Z*,2*E*)-but-2-enal phthalazin-1-ylhydrazone **13**, (6%, mp 83–85 °C). ν_{max}(nujol)/cm^{-1} 3170 (NH), 1633 (C=N), 1604 and 1591 (C=C); δ_H (600 MHz; $CDCl_3$; Me_4Si) 1.87 [3 H, dd, $J_{2,4}$ 1.5 $J_{3,4}$ 6.9, C(4)H], 6.16 [1 H, dq, $J_{2,3}$ 15.3 $J_{3,4}$ 6.9, H(3)], 7.21 [1 H, ddq, $J_{1,2}$ 9.6 $J_{2,3}$ 15.3 $J_{2,4}$ 1.5, C(2)H], 7.32 [1 H, d, $J_{1,2}$ 9.6, C(1)H], 7.39–7.42 [1 H, m, C(5′)H],

7.52–7.59 [2 H, m, C(6′,7′)H], 7.74 [1 H, s, C(4′)H], 8.32–8.35 [1 H, m, C(8′)H], 10.42 [1 H, br s, NH]; δ_C (150 MHz; $CDCl_3$; Me_4Si) 18.65 [C(4)], 123.16 [C(2)], 124.27 [C(8′)], 125.91 [C(5′)], 127.08 [C(8a′)], 127.32 [C(4a′)], 131.39 [C(7′)], 131.81 [C(6′)], 137.81 [C(4′)], 139.29 [C(3)], 147.54 [C(1′)], 154.01 [C(1)]; *m/z* (EI): 212.1068 ($M^{+\bullet}$, $C_{12}H_{12}N_4$ requires 212.1062), 197 (100%), 171 (23).

Reaction kinetics of hydralazine with acrolein and crotonaldehyde

To determine whether kinetic or stability factors contribute to the different hydrazone yields during the reaction of hydralazine with **1** and **2**, the time-course of hydrazone formation was explored under the same reaction conditions used in determining the 2-alkenal scavenging potential of **3**, except that reactions were followed for up to 24 h. Also, to explore the role of reaction temperature in product yields and stability, the reactions were performed in parallel at 37 and 4 °C. At 10 min, 30 min, 2 h, 3 h, 4 h, 6 h, 12 h and 24 h, aliquots of reaction mixture were removed for the determination of reaction products and starting materials *via* HPLC. The formation of the high R_f products of hydralazine with **3** and **2**, *E*-APH **10** and *E*-BPH **12** respectively, were measured at 210 nm on a Zorbax Eclipse XDB C18 column (250 × 4.6 mm) with a 5 μm particle size (Agilent Technologies, USA) using the HPLC system mentioned above. The mobile phase (30% acetonitrile in sodium phosphate buffer [50 mM, pH 7] and 40% acetonitrile in sodium phosphate buffer for compound **10** and product **12** respectively) was pumped at a flow rate of 1 mL min^{-1}. The retention times for product **10** and compound **12** with their respective mobile phases were 17.0 and 13.1 min. The stability of compounds **1**, **2**, **10** and **12** in the reaction buffer in the absence of other reagents was also assessed at 37 °C and 4 °C. Free aldehydes were measured using the assays previously mentioned.

Protection against acrolein and crotonaldehyde-mediated toxicity

Hepatocytes were isolated *via* collagenase digestion of the livers of anaesthetised mice and plated at a density of 1×10^6 cells mL^{-1} on collagen-coated dishes (60 mm diameter, IWAKI, Japan, 3 mL cell suspension per plate).[32] Cells were allowed to attach to the dishes for 2 to 3 h in a humidified atmosphere of 5% CO_2 and 95% air at 37 °C before use. Dishes were then washed with 3 mL PBS (50 mM, pH 7.4) to remove nonadherent cells before they were incubated with either culture media alone or supplemented with one of the scavengers (1–100 μM; hydralazine **3**, dihydralazine **4**, aminoguanidine **5**, carnosine **6**, pyridoxamine **7**, methoxyamine **8**, MESNA **9**) for 5 min prior to the addition of allyl alcohol (100 μM) or crotyl alcohol (500 μM). All drugs and unsaturated alcohols were dissolved directly in culture media. Dishes were then returned to the incubator for 3 h with aliquots of culture media taken at 1 hourly intervals to assess lactate dehydrogenase (LDH) leakage from the cytoplasm. LDH activity in culture media was assayed using the method of Richards *et al.*,[33] adapted to the use of a fluorescence microplate reader (POLARStar, BMG Laboratories).

Detection of *E*-APH in the culture media of mouse hepatocytes

Mouse hepatocyte monolayers, prepared as outlined in the preceding section, were co-treated for 30 min with allyl alcohol (100 μM) and hydralazine **3** (0–100 μM) at 37 °C. Next, cells were ruptured by the addition of Triton® X-100 (0.3 mL, to give a final concentration of 0.5% v/v) followed by sonication to provide a whole dish lysate. The mixture was transferred to a centrifuge tube and then centrifuged at 1600 × *g* for 5 min to pellet cellular debris. The resulting supernatant was then applied to a solid phase extraction column (1 mL, C-18 packing; J. T. Baker Chemical Co., NJ, USA) that had been pre-equilibrated with tetrahydrofuran and then water. The column was then washed with water (1 mL) to remove buffer salts and residual hydralazine. Finally, APH was eluted with 300 μL tetrahydrofuran and the resulting eluant was diluted 1 : 1 in water before a 100 μL aliquot was analysed *via* HPLC for the presence of *E*-APH **10**. The method employed the Zorbax Eclipse XDB C-18 column and apparatus described above, except that the mobile phase comprised 40% acetonitrile/0.01% triethylamine in 50 mM sodium phosphate buffer (pH 7) at a flow rate of 1.2 mL min^{-1}.

Metabolism and toxicity of APH in mouse hepatocytes

Hepatocyte monolayers were exposed to 1 μM *E*-APH **10** for up to 3 h. At 30, 60, 120 and 180 min following the addition of **10**, dishes were removed from the incubator and Triton® X-100 was added to the supernatant and cell lysates were prepared as outlined above. Following the isolation of extracts on SPE columns, concentrations of **10** were determined in the samples *via* UV-HPLC as described above. In a related experiment, to determine whether trapping of **1** by **3** truly constitutes detoxication, the toxic potential of **10** was assessed by exposing mouse hepatocytes to 1 to 100 μM concentrations of **10**, and aliquots of culture media were taken for the assessment of LDH leakage at 60, 120 and 180 min.

Acknowledgements

The authors are grateful for financial support received from the Medical Research Committee of the Faculty of Health Sciences at the University of Adelaide.

References

1 M. L. Selley, M. R. Bartlett, J. A. McGuiness, A. J. Hapel, N. G. Ardlie and M. J. Lacey, *J. Chromatogr.*, 1989, **488**, 329–340.
2 B. Andrews, K. Burnand, G. Paganga, N. Browse, C. Rice-Evans, K. Sommerville, D. Leake and N. Taub, *Atherosclerosis*, 1995, **112**, 77–84.
3 K. Uchida, M. Kanematsu, K. Sakai, T. Matsuda, N. Hattori, Y. Mizuno, D. Suzuki, T. Miyata, N. Noguchi, E. Niki and T. Osawa, *Proc. Natl. Acad. Sci. USA*, 1998, **95**, 4882–4887.
4 Y. He, M. Nagano, H. Yamamoto, E. Miyamoto and M. Futatsuka, *Drug Chem. Toxicol.*, 1995, **18**, 315–331.
5 J. Newcombe, H. Li and M. L. Cuzner, *Neuropathol. Appl. Neurobiol.*, 1994, **20**, 152–162.
6 M. A. Lovell, C. Xie and W. R. Markesbery, *Neurobiol. Aging*, 2001, **22**, 187–194.
7 D. Suzuki, T. Miyata, N. Saotome, K. Horie, R. Inagi, Y. Yasuda, K. Uchida, Y. Izuhara, M. Yagame, H. Sakai and K. Kurokawa, *J. Am. Soc. Nephrol.*, 1999, **10**, 822–832.
8 H. Esterbauer, R. J. Schaur and H. Zollner, *Free Radical Biol. Med.*, 1991, **11**, 81–128.
9 A. Zlatkis, C. F. Poole, R. Brazeli, D. A. Bafus and P. S. Spencer, *J. Chromatogr.*, 1980, **182**, 137–145.
10 C. J. Kensler and S. P. Battista, *New Eng. J. Med.*, 1963, **269**, 1161–1166.
11 C. Izard and C. Libermann, *Mutat. Res.*, 1978, **47**, 115–138.
12 N. Y. Calingasan, K. Uchida and G. E. Gibson, *J. Neurochem.*, 1999, **72**, 751–756.
13 D. Suzuki, T. Miyata, N. Saotome, K. Horie, R. Inagi, Y. Yasuda, K. Uchida, Y. Izuhara, M. Yagame, H. Sakai and K. Kurokawa, *J. Am. Soc. Nephrol.*, 1999, **10**, 822–832.
14 P. C. Burcham, P. G. Kerr and F. Fontaine, *Redox Rep.*, 2000, **5**, 47–49.
15 P. C. Burcham, L. M. Kaminskas, F. R. Fontaine, D. R. Petersen and S. M. Pyke, *Toxicology*, 2002, **181–182**, 229–236.
16 H. K. Shapiro, *Am. J. Therap.*, 1998, **5**, 323–353.
17 M. Brownlee, H. Vlassara, A. Kooney, P. Ulrich and A. Cerami, *Science*, 1986, **232**, 1629–1632.
18 Y. Al-Abed and R. Bucala, *Chem. Res. Toxicol.*, 1997, **10**, 875–879.
19 G. Aldini, P. Granata and M. Carini, *J. Mass Spectrom.*, 2002, **37**, 1219–1228.
20 G. Aldini, M. Carini, G. Beretta, S. Bradamante and R. M. Facino, *Biochem. Biophys. Res. Commun.*, 2002, **298**, 699–706.
21 S. Zhou and E. A. Decker, *J. Agric. Food Chem.*, 1999, **47**, 51–55.
22 A. R. Hipkiss, V. C. Worthington, D. T. Himsworth and W. Herwig, *Biochim. Biophys. Acta*, 1998, **1380**, 46–54.

23 J. M. Onorato, A. J. Jenkins, S. R. Thorpe and J. W. Baynes, *J. Biol. Chem.*, 2002, **275**, 21177–21184.
24 P. A. Reece, *Med. Res. Rev.*, 1981, **1**, 73–96.
25 P. A. Reece, I. Cozamanis and R. Zacest, *J. Chromatogr.*, 1980, **181**, 427–440.
26 B. O. Nilsson, *Inflamm. Res.*, 1999, **48**, 509–515.
27 F. Fontaine, R. A. Dunlop, D. R. Petersen and P. C. Burcham, *Chem. Res. Toxicol.*, 2002, **15**, 1051–1058.
28 L. E. Rikans, *Drug Metab. Dispos.*, 1987, **15**, 356–362.
29 P. C. Burcham and F. R. Fontaine, *J. Biochem. Mol. Toxicol.*, 2001, **15**, 309–316.
30 N. Brock, J. Pohl, J. Stekar and W. Scheef, *Eur. J. Cancer Clin. Oncol*, 1982, **18**, 1377–1387.
31 F. Serafini-Cessi, *Biochemistry*, 1972, **128**, 1103–1107.
32 A. W. Harman, L. E. McCamish and C. A. Henry, *J. Pharmacol. Methods*, 1987, **17**, 157–163.
33 A. H. Richards, R. M. Lubinski and R. E. Vanderlinde, *Clin. Chem.*, 1975, **21**, 1018–1023.